Peak shifts due to $B^{(*)} - \bar{B}^{(*)}$ rescattering in $\Upsilon(5S)$ dipion transitions

Ce Meng[1] and Kuang-Ta Chao[1,2]

[1]*Department of Physics and State Key Laboratory of Nuclear Physics and Technology, Peking University, Beijing 100871, China*
[2]*Center for High Energy Physics, Peking University, Beijing 100871, China*

We study the energy distributions of dipion transitions $\Upsilon(5S)$ to $\Upsilon(1S, 2S, 3S)\pi^+\pi^-$ in the final-state rescattering model. Since the $\Upsilon(5S)$ is well above the open bottom thresholds, the dipion transitions are expected to mainly proceed through the real processes $\Upsilon(5S) \to B^{(*)}\bar{B}^{(*)}$ and $B^{(*)}\bar{B}^{(*)} \to \Upsilon(1S, 2S, 3S)\pi^+\pi^-$. We find that the energy distributions of $\Upsilon(1S, 2S, 3S)\pi^+\pi^-$ markedly differ from that of $\Upsilon(5S) \to B^{(*)}\bar{B}^{(*)}$. In particular, the resonance peak will be pushed up by about 7–20 MeV for these dipion transitions relative to the main hadronic decay modes. These predictions can be used to test the final-state rescattering mechanism in hadronic transitions for heavy quarkonia above the open flavor thresholds.

I. INTRODUCTION

Hadronic transitions between heavy quarkonia are important for understanding both the heavy quarkonium dynamics and the formation of light hadrons (for recent reviews see, e.g. [1]). Particularly, in recent years, the dipion and single pion transitions have proved to be a very efficient way to discover new or missing charmonium or charmoniumlike states, the so-called "*X, Y, Z*" mesons, by Belle, Babar, and CLEO collaborations (see [2] for a recent review and related references). To search for the partners of *X* and *Y* in the $b\bar{b}$ sector, say X_b and Y_b, a similar approach was also suggested [3]. More recently, Belle has found a very striking result [4] that signals of $\Upsilon(mS)\pi^+\pi^-$ with $m = 1, 2, 3$ collected at the energy of 10 870 MeV, i.e. at the peak of $\Upsilon(5S)$, indicate that the partial widths of $\Upsilon(5S) \to \Upsilon(mS)\pi^+\pi^-$ are larger than that of $\Upsilon(4S) \to \Upsilon(1S, 2S)\pi^+\pi^-$ by 2 orders of magnitude or more if the $\Upsilon(5S)$ is the sole source of the observed dipion transition events.

If the peak at $\Upsilon(10\,870)$ is identified with the $\Upsilon(5S)$ resonance, we will have to answer the question: what is the essential difference between the $\Upsilon(5S)$ and $\Upsilon(4S)$ in their dipion transitions. To answer this question, in an earlier paper [5] we use the final-state rescattering model [6] to study the dipion transitions of $\Upsilon(5S)$ and $\Upsilon(4S)$. In this model, the $\Upsilon(5S/4S)$ first decays to $B^{(*)}\bar{B}^{(*)}$, and then the B meson pair turns into a lower Υ state and two pions through exchange of another $B^{(*)}$ meson. Since the real rescattering contributions are expected to be dominant in these processes, the difference between $\Upsilon(5S)$ and $\Upsilon(4S)$ dipion transitions can be explained mainly by the difference in available phase space for the $\Upsilon(5S/4S) \to B^{(*)}\bar{B}^{(*)}$ decays. Although sharing the same quantum numbers and having similar leptonic widths, the $\Upsilon(5S)$ and $\Upsilon(4S)$ are dramatically different in their hadronic transitions. In the real rescattering process where the $b\bar{b}$ resonance is above the open bottom threshold, the amplitude is basically propor-

tional to the probability of the corresponding open bottom decay, which is proportional to the P-wave phase space factor $|\vec{p}_1|^3$ [5,7]. Here, $\vec{p}_1$ denotes the 3-momentum of $B^{(*)}$ or $\bar{B}^{(*)}$ in the rest frame of $\Upsilon(5S/4S)$. Note that the *p* value $|\vec{p}_1|$ of the decay $\Upsilon(5S) \to B\bar{B}$ is about 3.84 times larger than that of $\Upsilon(4S) \to B\bar{B}$, and this fact will mainly result in a huge difference, which is about a factor of 200–600 in magnitude [5], between the partial widths of dipion transitions of $\Upsilon(5S)$ and $\Upsilon(4S)$. (Note that the $|\vec{p}_1|^6$ factor would give an enhancement of about 3200 for the $\Upsilon(5S)$ relative to $\Upsilon(4S)$ but an effective form factor associated with the coupling constants will lower the enhancement factor by about an order of magnitude; see discussions in next sections.) As a result of the rescattering mechanism, it might be unnecessary to introduce an exotic interpretation of $\Upsilon(5S)$ resonance or a Y_b state to account for the experimental data [4].

To further clarify the issue mentioned above, it is useful to study other features of the final-state rescattering mechanism. In this paper, we will show that a distinct and important consequence of the final-state rescattering mechanism is the peak shift effect, which is related to the unique energy dependence of the cross section of $e^+e^- \to \Upsilon(5S) \to \Upsilon(mS)\pi^+\pi^-$. As a result of the final-state rescattering process $B^{(*)}\bar{B}^{(*)} \to \Upsilon(mS)\pi^+\pi^-$, the energy distributions of the $\Upsilon(5S) \to \Upsilon(mS)\pi^+\pi^-$ events will differ from that of $\Upsilon(5S) \to B^{(*)}\bar{B}^{(*)}$. In particular, the observed resonance peak in $\Upsilon(5S) \to \Upsilon(mS)\pi^+\pi^-$ is expected to be pushed up to higher energies markedly compared with that of $\Upsilon(5S) \to B^{(*)}\bar{B}^{(*)}$. The physical reason for this peak shift is quite evident that at higher energies around the $\Upsilon(5S)$ resonance peak the rescattering process will acquire more phase space and then get a larger rate. This peak shift effect is an inevitable result of the final-state rescattering, and therefore it can serve as a crucial test for this mechanism. In the following, we will study this effect in a more quantitative way.

II. THE RESCATTERING MODEL

As in Ref. [5], we assume that in the $\Upsilon(4S, 5S)$ dipion transitions the two pions are produced mainly via scalar resonances coupled to intermediate $B^{(*)}$ mesons due to the long-distance final-state interactions. The typical rescattering diagrams for $\Upsilon(4S, 5S) \to \Upsilon(1S, 2S)\mathcal{S}$ are shown in Fig. 1, and the others can be related to those in Fig. 1 by charge conjugation transformation $B \leftrightarrow \bar{B}$ and isospin transformation $B^0 \leftrightarrow B^+$ and $\bar{B}^0 \leftrightarrow B^-$. Here, $\mathcal{S}$ denotes scalar resonance σ or $f_0(980)$ (perhaps also $f_0(1370)$), which will decay to $\pi\pi(K\bar{K})$ eventually.

In Fig. 1, the intermediate states $B^{(*)}\bar{B}^{(*)}$ can be real or virtual, which corresponds, respectively, to the imaginary part or the real part of the amplitude. In Ref. [5], we argued that in general it is the real rescattering process that is dominant unless the resonance is very close to the open flavor threshold. More quantitatively, we used the dispersion relation to estimate the virtual rescattering contributions and found that they are extremely small for $\Upsilon(5S)$ because $\Upsilon(5S)$ is far above the $B\bar{B}$ threshold, whereas for $\Upsilon(4S)$, they can be comparable to the real ones but with large uncertainties [5]. Nevertheless, this does not affect the calculated large difference between the transition widths of $\Upsilon(5S)$ and $\Upsilon(4S)$. (In contrast, in the case of $X(3872)$ [8] or $Z(4430)$ [9], the virtual rescattering effects could be dominant due to the extreme closeness between the resonance mass and the open flavor threshold.)

In the real rescattering processes, the amplitudes of Fig. 1(a)–1(d) are dominated by their absorptive (imaginary) parts, which can be derived by the Cutkosky rule as [5]
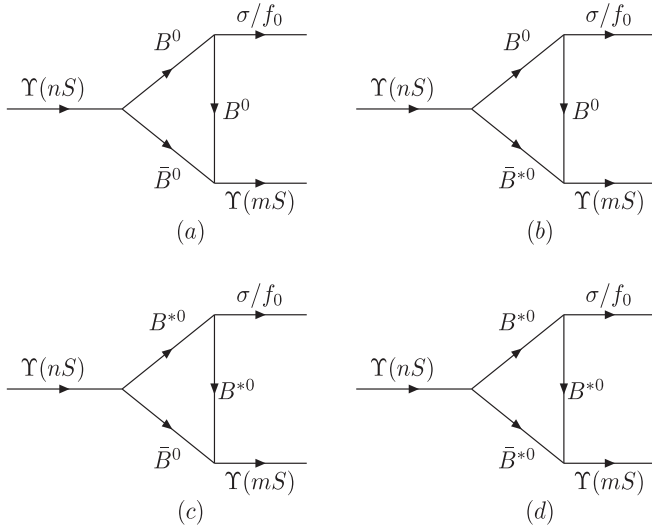

FIG. 1.   Typical diagrams for $\Upsilon(nS) \to B^{(*)}\bar{B}^{(*)} \to \Upsilon(mS)\mathcal{S}$. Other diagrams can be obtained by charge conjugation transformation $B \leftrightarrow \bar{B}$ and isospin transformation $B^0 \leftrightarrow B^+$ and $\bar{B}^0 \leftrightarrow B^-$.

$$\mathbf{Abs}_i = \frac{|\vec{p}_1|}{32\pi^2 m_{\Upsilon(nS)}} \int d\Omega \, \mathcal{A}_i(\Upsilon(nS)$$
$$\to B^{(*)}\bar{B}^{(*)})\mathcal{C}_i(B^{(*)}\bar{B}^{(*)} \to \Upsilon(mS)\mathcal{S}), \quad (1)$$

where $i = (a, b, c, d)$, and $d\Omega$ and $\vec{p}_1$ denote the solid angle of the on shell $B^{(*)}\bar{B}^{(*)}$ system and the 3-momentum of the on shell $B^{(*)}$ meson in the rest frame of $\Upsilon(nS)$, respectively.

The amplitudes $\mathcal{A}_i$ and $\mathcal{C}_i$ are determined by the effective Lagrangians [5]

$$\mathcal{L}_{\Upsilon BB} = g_{\Upsilon BB}\Upsilon_\mu(\partial^\mu BB^\dagger - B\partial^\mu B^\dagger), \quad (2a)$$

$$\mathcal{L}_{\Upsilon B^*B} = \frac{g_{\Upsilon B^*B}}{m_\Upsilon}\varepsilon^{\mu\nu\alpha\beta}\partial_\mu\Upsilon_\nu(B^*_\alpha\overset{\leftrightarrow}{\partial}_\beta B^\dagger - B\overset{\leftrightarrow}{\partial}_\beta B^{*\dagger}_\alpha), \quad (2b)$$

$$\mathcal{L}_{\Upsilon B^*B^*} = g_{\Upsilon B^*B^*}(-\Upsilon^\mu B^{*\nu}\overset{\leftrightarrow}{\partial}_\mu B^{*\dagger}_\nu + \Upsilon^\mu B^{*\nu}\partial_\nu B^{*\dagger}_\mu$$
$$- \Upsilon_\mu\partial_\nu B^{*\mu}B^{*\nu\dagger}), \quad (2c)$$

$$\mathcal{L}_{SBB} = g_{SBB}SBB^\dagger, \quad (2d)$$

$$\mathcal{L}_{SB^*B^*} = -g_{SB^*B^*}SB^* \cdot B^{*\dagger}, \quad (2e)$$

where $\overset{\leftrightarrow}{\partial} = \overset{\rightarrow}{\partial} - \overset{\leftarrow}{\partial}$. Here, the heavy quark symmetry and chiral symmetry in (2) are basically ensured by the kinematic conditions.

Following Ref. [5], we choose the on shell coupling constants

$$g_{\Upsilon(mS)B^{(*)}B^{(*)}} = 24, \qquad m \leq 4 \quad (3)$$

$$g_{\Upsilon(5S)BB} = 2.5, \quad (4)$$

$$g_{\Upsilon(5S)B^*B} = 1.4 \pm 0.3, \quad (5)$$

$$g_{\Upsilon(5S)B^*B^*} = 2.5 \pm 0.4, \quad (6)$$

where the values in (3)–(6) are determined by the measured widths $\Gamma(\Upsilon(4S) \to B\bar{B})$ and $\Gamma(\Upsilon(5S) \to B^{(*)}\bar{B}^{(*)})$, respectively. On the other hand, the coupling constants $g_{SB^{(*)}B^{(*)}}$ can be related to the well-known one $g_{D^*D\pi}$ [8] by heavy quark flavor symmetry and chiral symmetry, and we choose [5]

$$g_{\sigma BB} = g_{\sigma B^*B^*} = 10 \text{ GeV},$$

$$g_{f0BB} = g_{f0B^*B^*} = 10\sqrt{2} \text{ GeV}.$$

To account for the off shell effect of the exchanged $B^{(*)}$ meson in Fig. 1, one need introduce form factors, such as [6]

$$\mathcal{F}_1(m_i, q^2) = \frac{(\Lambda + m_i)^2 - m_i^2}{(\Lambda + m_i)^2 - q^2}, \quad (7)$$

to the vertexes SBB and $\Upsilon(mS)BB$. We will fix the cutoff $\Lambda = 660$ MeV [5] in our numerical analysis in the next section.

We treat the scalar resonance $\mathcal{S}$ as a narrow one and use the Breit-Wigner distribution

TABLE I.   Resonance parameters of σ and $f_0(980)$ [10,11].

	m_S (MeV)	$g_{S\pi\pi}$ (GeV)	$\Gamma_{S\pi\pi}$ (MeV)	g_{SKK} (GeV)	Γ_{SKK} (MeV)
σ	526 ± 30	3.06	302 ± 10		
$f_0(980)$	980 ± 10	1.77	61 ± 1	2.70	12 ± 1

$$\mathcal{F}_S(t) = \frac{1}{\pi} \frac{\sqrt{t}\Gamma_S(t)}{(t - m_S^2)^2 + m_S^2\Gamma_S(t)^2} \tag{8}$$

to describe the resonance in the calculation of cross sections, as the treatment of ρ resonance in Ref. [8]. In (8), the variable t denotes the momentum squared of $\mathcal{S}$, and the function $\Gamma_S(t)$ is given by

$$\Gamma_S(t) = \frac{p_\pi g_{S\pi\pi}}{8\pi t} + \frac{p_K g_{SKK}}{8\pi t}, \qquad p_\pi = \sqrt{\frac{t}{4} - m_\pi^2}, \qquad p_K = \sqrt{\frac{t}{4} - m_K^2}. \tag{9}$$

The resonance parameters in (8) and the coupling constants in (9), which are listed in Table I, are chosen mostly from Ref. [11], except for $m_{f_0(980)}$ from PDG2006 [10].

Although the Breit-Wigner description (8) for the scalar resonance is somehow rough, especially for the σ, it is efficient enough to get the order of magnitude of the widths $\Gamma(\Upsilon(4S/5S) \rightarrow \Upsilon(mS)\pi\pi)$ correctly [5]. Moreover, since the final-state phase space (FSPS) of $\Upsilon(5S) \rightarrow \Upsilon(mS)\mathcal{S}$ is smeared by the large width of $\mathcal{S}$, one would not expect that this FSPS could bring on large energy dependence of the cross section, unless it happens to be near the threshold, such as the case of $\Upsilon(5S) \rightarrow \Upsilon(3S)\sigma$. We will discuss this further in the next section.

III. PEAK SHIFTS IN $\Upsilon(5S)$ DIPION TRANSITIONS

In the absorptive part **Abs**$_i$ in (1), the amplitude $\mathcal{A}_i$ is proportional to $|\vec{p}_1|$ since it involves an on shell P-wave vertex $\Upsilon(nS)B^{(*)}B^{(*)}$. Furthermore, a hidden factor $|\vec{p}_1|$ will emerge after performing the integral in (1) explicitly. As a result, the amplitude **Abs**$_i$ is proportional to $|\vec{p}_1|^3$. As we have mentioned above, this brings on the strong s dependence of the cross section of $e^+e^- \rightarrow \Upsilon(5S) \rightarrow B^{(*)}\bar{B}^{(*)} \rightarrow \Upsilon(mS)\pi^+\pi^-$, and may change the distribution of the $\Upsilon(mS)\pi^+\pi^-$ signals significantly around the peak of $\Upsilon(5S)$ resonance.

In general, neglecting radiative corrections and the beam-energy spread, the cross section for the process $e^+e^- \rightarrow$ resonance $r \rightarrow$ hadronic final state f at the center-of-mass energy $\sqrt{s}$ can be approximately expressed by the Breit-Wigner form

$$\sigma(s) = 12\pi \frac{\Gamma_r^{ee} \cdot \Gamma_r^f(s)}{(s - m_r^2)^2 + m_r^2\Gamma_r(s)^2}, \tag{10}$$

where the resonance r is parameterized by its mass m_r, the total width Γ_r, the electronic width Γ_r^{ee}, and the partial

width Γ_r^f for the decay channel f. For the $\Upsilon(5S)$, in (10) we have neglected the weak s dependence of m_r, Γ_r^{ee}. However, for the final states $f = \Upsilon(1S/2S/3S)\pi^+\pi^-$, the s dependence of Γ_r^f is as strong as $|\vec{p}_1(s)|^6$, and therefore cannot be neglected at all.

As a first step, we will neglect the energy dependence of the total width of $\Upsilon(5S)$ as well. Thus, for the final state, such as $f =$ light hadrons, the energy distribution of the cross section of $\Upsilon(5S)$ will peak at m_{5S} exactly as that shown in Fig. 2 by the dashed line. We call this the naive Breit-Wigner distribution. In Fig. 2, the resonance parameters of $\Upsilon(5S)$ have been chosen from PDG2006 [10] with the following central values of m_{5S} and Γ_{5S}:

$$m_{5S} = 10\,865 \text{ MeV}, \qquad \Gamma_{5S} = 110 \text{ MeV}. \tag{11}$$

Then, we can compare the naive Breit-Wigner distribution with the one where $\Gamma_{5S}^f(s) \sim |\vec{p}_1(s)|^6$. For the $B\bar{B}$ intermediate state, the result is shown in Fig. 2 with the solid line. One can see that the strong s dependence of Γ_{5S}^f pushes the resonance peak up with a energy shift of about 15 MeV.

The two-body decay modes $B^{(*)}\bar{B}^{(*)}$ and $B_s^{(*)}\bar{B}_s^{(*)}$, which are dominant ones of $\Upsilon(5S)$ [10], will bring on large energy dependence of Γ_{5S} and change the distributions in Fig. 2 consequently. For simplicity, we will choose the main decay mode $B^*\bar{B}^*$ to estimate the energy dependence of
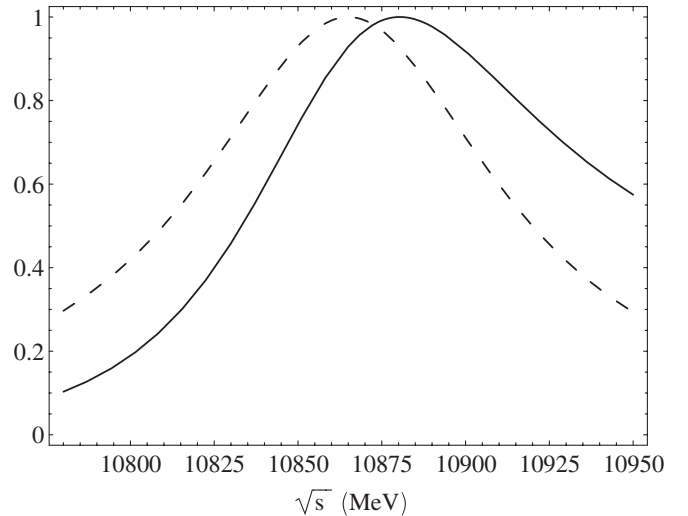

FIG. 2.   Resonance line shapes of the naive Breit-Wigner distribution (dashed line) and the one with $\Gamma_r^f(s) \sim |\vec{p}_1(s)|^6$ and $B\bar{B}$ as the intermediate state (solid line). The maximums are normalized to one, respectively.

Γ_{5S}. That is,

$$\Gamma_{5S}(s) \sim \Gamma_{5S}^{B^*\bar{B}^*}(s) \sim \frac{s + 3m_{B^*}^2}{s}\left(\frac{\sqrt{s - 4m_{B^*}^2}}{2}\right)^3, \quad (12)$$

which can be derived from the effective Lagrangian (2c) with $g_{\Upsilon(5S)B^*B^*}$ being treated as a constant independent of s. Here, $\Gamma_{5S}(m_{5S})$ is normalized to be 110 MeV, like that in (11).

Furthermore, one need introduce form factors for every $\Upsilon(5S)B^{(*)}\bar{B}^{(*)}$ vertex in Fig. 1. Following Ref. [12], we choose the form factor

$$\mathcal{F}(s) = \frac{\exp(-\alpha|\vec{p}_1(s)|^2)}{\exp(-\alpha|\vec{p}_1(m_{5S}^2)|^2)}, \quad (13)$$

which is normalized to 1 at $s = m_{5S}^2$, since we have extracted the on shell coupling constants $g_{\Upsilon(5S)B^{(*)}\bar{B}^{(*)}}$ in (4)–(6) at this energy point. This form factor, which is associated with the effective $\Upsilon(5S)B^{(*)}\bar{B}^{(*)}$ coupling, can be understood as the consequence of the overlap integral of the wave functions of $\Upsilon(5S)$ and the two $B^{(*)}$ mesons, and the scale factor α can be related to the effective radius of the interaction, R, by $\alpha = R^2/6$ [12]. It is this form factor (or others of a similar form) that plays the role to naturally balance the otherwise over-increased decay rates with increased phase space. Namely, this form factor is a sort of "cutoff" for the high momentum of the final-state mesons. The momentum dependence of the effective couplings can partially explain why the coupling constants $g_{\Upsilon(5S)B^{(*)}\bar{B}^{(*)}}$ are smaller than the one $g_{\Upsilon(4S)BB}$, though for $\alpha = 0$–1 GeV^{-2} the suppression from the form factor is not strong enough to account for the large difference between the values in (3) and in (4)–(6). This suppression may be additionally due to the node structure of the wave function of highly excited $\Upsilon(5S)$ [5].

Needless to say, the form factor in (13) should also change the energy dependence of the width $\Gamma_{5S}^{B^{(*)}\bar{B}^{(*)}}(s)$ and the total width $\Gamma_{5S}(s)$ in (12) subsequently. Such α dependence of $\Gamma_{5S}(s)$ is shown in Fig. 3. One can see that the energy dependence is significantly weakened when α is about 0.6 GeV^{-2} (solid line in Fig. 3). As a result, the distribution of $\Upsilon(5S)$ with $f = B^*\bar{B}^*$ and $\alpha = 0.6$ GeV^{-2}, which is shown in Fig. 4 with the dashed line, is very close to the naive Breit-Wigner one.

With $\alpha = 0.6$ GeV^{-2} [12], the distributions for $f = \Upsilon(1S)\pi^+\pi^-$ can be evaluated numerically. Since here we only focus on the line shape and the peak shift, which are almost independent of the parameters except α and $\Gamma_{5S}(m_{5S})$, it is quite safe to choose the central values for other parameters introduced in the last section. The distribution for $f = \Upsilon(1S)\pi^+\pi^-$ is illustrated in Fig. 4 with the solid line. Compared with the distribution for $f = B^*\bar{B}^*$ (the dashed line), the peak shift is about 7 MeV. If we choose the channel $B\bar{B}$ as the main hadronic channel, the
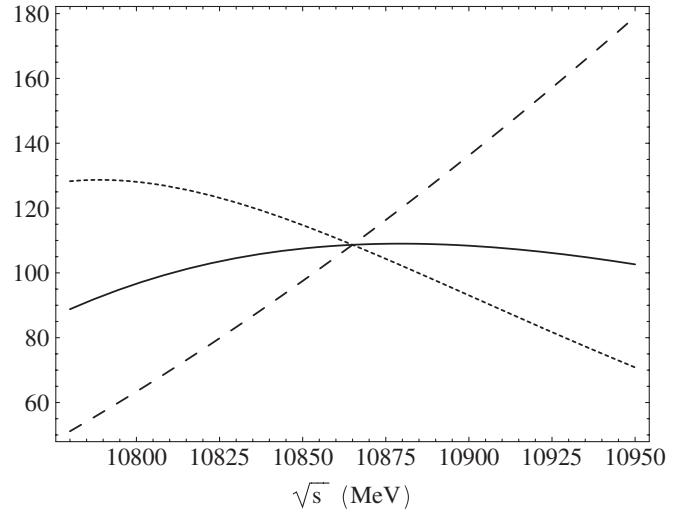

FIG. 3.   The energy dependence and α dependence of $\Gamma_{5S}(s)$. The dashed line, solid line, and dotted line are evaluated with $\alpha = 0.0$, 0.6 and 1.0 GeV^{-2}, respectively.

peak shift can be as large as 11 MeV for the $\Upsilon(1S)\pi^+\pi^-$ channel.

The energy distribution for $f = \Upsilon(2S)\pi^+\pi^-$ has similar line shape to that for $f = \Upsilon(1S)\pi^+\pi^-$ within the energy region of 10 780–10 950 MeV. Furthermore, since the transition $\Upsilon(5S) \to \Upsilon(3S)\pi^+\pi^-$ is also observed [4] with a large rate and quite high statistical significance (3.2σ), we also evaluate its energy distribution in Fig. 4 with the dotted line. We find there is an additional peak shift of about 12 MeV relative to the distribution for $f = \Upsilon(1S)\pi^+\pi^-$. This is just because the role of the scalar resonance in Fig. 1. In our model [5], the final-state $\pi^+\pi^-$ are assumed to be dominated by the scalar resonance
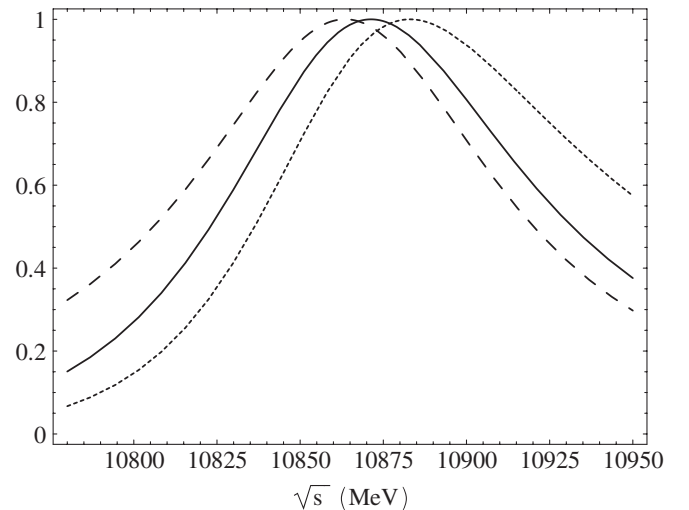

FIG. 4.   Resonance line shapes for $f = B^*\bar{B}^*$ (dashed line) and the one for $f = \Upsilon(1S)\pi^+\pi^-$ (solid line), and for $f = \Upsilon(3S)\pi^+\pi^-$ (dotted line) with $\alpha = 0.6$ GeV^{-2}. The maximums are normalized to one, respectively.

$\mathcal{S}(\sigma, f_0(980)\ldots)$ [11], which can be described by the Breit-Wigner distribution (8) at the cross section level. If the mass of the σ resonance is chosen as $m_\sigma = 526$ MeV given in Table I, then one can easily find that the mass difference $m_{5S} - m_{3S} \approx 510$ MeV happens to be in the center of the distribution in (8). As we have mentioned in the end of the last section, this brings on another strong s dependence to the cross section for $f = \Upsilon(3S)\sigma(\pi^+\pi^-)$. Thus, the distribution for $f = \Upsilon(3S)\pi^+\pi^-$ is pushed up farther than those for $f = \Upsilon(1S, 2S)\pi^+\pi^-$. Similarly, there will be a long tail in the distribution for $f = \Upsilon(2S)\pi^+\pi^-$ within the energy region of 10 950–11 100 MeV due to the emergence of the scalar resonance $f_0(980)$.

It is worth emphasizing that the scalar resonance dominance is just a simplification to study the effects of the final-state rescattering mechanism in the $\Upsilon(5S) \rightarrow \Upsilon(1S, 2S, 3S)\pi^+\pi^-$ transitions [5]. Thus, the differences between the distributions for $f = \Upsilon(1S, 2S, 3S)\pi^+\pi^-$ tend to disappear if the nonresonance contributions and their interference with the scalar resonances are important. Therefore, to detect the differences between the distributions for $f = \Upsilon(1S, 2S, 3S)\pi^+\pi^-$ can provide useful information on the role of the scalar resonances in these transitions. More valuable information can also be given by the measurements on the $M(\pi\pi)$ spectrum and the distribution of the helicity angle [4].

It is obvious that the position of the resonance peaks of $\Upsilon(5S)$ in $\Upsilon(1S, 2S, 3S)\pi^+\pi^-$ channels depend on the value of the scale factor α in the form factor (13). However, the energy distributions of $\Upsilon(5S)$ in other main hadronic decay channels (e.g., $B\bar{B}\ldots$) also depend on the same factor α. So, it is essential to compare the line shape for, e.g., $f = \Upsilon(1S)\pi^+\pi^-$ with those main hadronic decay channels with different choices of the value of the scale factor. For $\alpha = 0.0$–1.0 GeV^{-2}, the results are shown in Fig. 5, where the $B^*\bar{B}^*$ channel is used to serve as one of the main hadronic channels again.

In Fig. 5, with a reasonable choice for the cutoff factor α, say, 0.3–0.8 GeV^{-2}, the relative peak shifts for $f = \Upsilon(1S, 3S)\pi^+\pi^-$ are found to be almost independent of the cutoff. Thus, we incline to conclude that there should be a peak shift of about 7 MeV for the distribution of $\Upsilon(5S)$ in the $\Upsilon(1S)\pi^+\pi^-$ channel compared with that in the $B^*\bar{B}^*$ channel. Similar shift should be obtained in the $\Upsilon(2S)\pi^+\pi^-$ channel. On the other hand, the shift in the $\Upsilon(3S)\pi^+\pi^-$ channel could be 12 MeV larger than those in
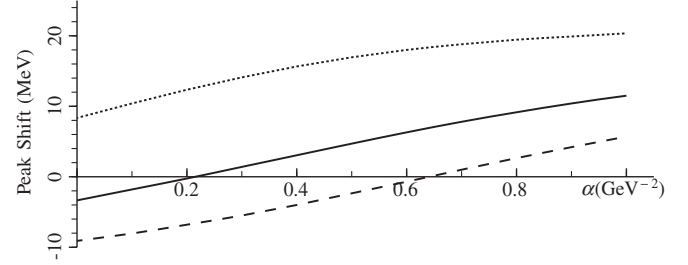

FIG. 5. α dependence of the peak shifts compared with $m_{5S} = 10\,865$ MeV for $f = B^*\bar{B}^*$ (dashed line), $f = \Upsilon(1S)\pi^+\pi^-$ (solid line), and $f = \Upsilon(3S)\pi^+\pi^-$ (dotted line).

the $\Upsilon(1S, 2S)\pi^+\pi^-$ channels, but this depends on the assumption that the scalar resonance σ dominates the $\Upsilon(3S)\pi^+\pi^-$ transition. Furthermore, if the $B\bar{B}$ is chosen as the main hadronic channel, the peak shifts will be enlarged by 3–4 MeV.

IV. SUMMARY

In summary, we study the energy distributions of dipion transitions $\Upsilon(5S)$ to $\Upsilon(1S, 2S, 3S)\pi^+\pi^-$ in the final-state rescattering model. Since the $\Upsilon(5S)$ is well above the open bottom thresholds, the dipion transitions can proceed through the real process $\Upsilon(5S) \rightarrow B^{(*)}\bar{B}^{(*)}$ and the subsequent process $B^{(*)}\bar{B}^{(*)} \rightarrow \Upsilon(1S, 2S, 3S)\pi^+\pi^-$. This model can not only explain the observed unusually large rates of $\Upsilon(5S) \rightarrow \Upsilon(1S, 2S, 3S)\pi^+\pi^-$ [5], but also predict a unique energy dependence of the cross sections of $e^+e^- \rightarrow \Upsilon(5S) \rightarrow \Upsilon(1S, 2S, 3S)\pi^+\pi^-$. We find that the energy distributions of $\Upsilon(1S, 2S, 3S)\pi^+\pi^-$ markedly differ from that of $\Upsilon(5S) \rightarrow B^{(*)}\bar{B}^{(*)}$, and, in particular, the resonance peak will be pushed up by about 7–20 MeV for these dipion transitions relative to the main hadronic decay modes. These predictions can be used to test the final-state rescattering mechanism in hadronic transitions for heavy quarkonia above the open flavor thresholds.

[1] Y. P. Kuang, Front. Phys. China **1,** 19 (2006); M. B. Voloshin, arXiv:0711.4556 [Prog. Part. Nucl. Phys. (to be published)]; E. Eichten, S. Godfrey, H. Mahlke, and J. L. Rosner, arXiv:hep-ph/0701208.

[2] S. L. Olsen, arXiv:0801.1153 [Chin. Phys. C (to be published)].

[3] W. S. Hou, Phys. Rev. D **74**, 017504 (2006).

[4] K. F. Chen *et al.* (Belle Collaboration), arXiv:0710.2577.

[5] C. Meng and K. T. Chao, Phys. Rev. D **77**, 074003 (2008).

[6] H. Y. Cheng, C. K. Chua, and A. Soni, Phys. Rev. D **71**, 014030 (2005); P. Colangelo, F. De Fazio, and T. N. Pham, Phys. Lett. B **542**, 71 (2002); Phys. Rev. D **69**, 054023 (2004); X. Liu, B. Zhang, and S. L. Zhu, Phys. Lett. B **645**, 185 (2007).

[7] Yu. A. Simonov, JETP Lett. **87**, 147 (2008); arXiv:0804.4635.

[8] C. Meng and K. T. Chao, Phys. Rev. D **75**, 114002 (2007).

[9] C. Meng and K. T. Chao, arXiv:0708.4222.

[10] W. M. Yao *et al.*, J. Phys. G **33**, 1 (2006); See also the web site http://pdg.lbl.gov/.

[11] T. Komada, M. Ishida, and S. Ishida, Phys. Lett. B **508**, 31 (2001); **518**, 47 (2001).

[12] M. R. Pennington and D. J. Wilson, Phys. Rev. D **76**, 077502 (2007).